



Received on 06 March, 2017; received in revised form, 29 April, 2017; accepted, 27 May, 2017; published 01 October, 2017

## PHYTO-FABRICATION OF SILVER NANOPARTICLES BY DIFFERENT PHYSICO-CHEMICAL PARAMETRES USING *PETREA VOLUBILIS* L. LEAF BROTH AND EVALUATION OF THEIR ANTI-MICROBIAL ACTIVITY

N. I. Hulkoti\* and T. C. Taranath

P.G. Department of Studies in Botany, Environmental Biology Laboratory, Karnatak University, Dharwad - 580003, Karnataka, India.

### Keywords:

*Petrea volubilis*,  
Silver nanoparticles,  
Anti-microbial activity, FTIR,  
Zeta potential, EDS, HR-TEM

### Correspondence to Author:

**Nasreen I Hulkoti**

Research Scholar,  
P.G. Department of Studies in  
Botany, Environmental Biology  
Laboratory, Karnatak University,  
Dharwad - 580003, Karnataka, India.


**E-mail:** nihnasreen@gmail.com

**ABSTRACT:** The present study instantiates the phyto-fabrication of silver nanoparticles by utilizing *Petrea volubilis* L. leaf broth which were instantaneously synthesised, eco-friendly, and cost-effective. The influence of physico-chemical parameters viz. contact time, leaf broth quantity, pH, temperature, and silver nitrate concentration were investigated and optimised to engineer infinitesimal nanoparticles. The SPR bands obtained from UV-vis spectroscopy confirmed the synthesis of silver nanoparticles. The active phytochemicals in *Petrea volubilis* L. leaf broth namely carboxylic acids, phenolic compounds and aldehydes were found to be responsible for the bio reduction and capping of silver ions according to FT-IR spectroscopy. The capping molecules of NPs were negatively charged and were passably stable as revealed by zeta potential measurements and the XRD patterns illustrated their crystallinity. HRTEM microphotographs enumerate spherical shaped nanoparticles. The EDS analysis at 20 confirms the synthesis of elemental silver. The nanoparticles were evaluated for their antimicrobial activity. The highest anti-bacterial activity was observed against *S. aureus* as compared to the bacteria *S. typhi* and *A. flavus* a fungus. The leaf extract did not show any anti-microbial activity. Our findings disclose the synthesis of various sizes of silver nanoparticles by varying the physico-chemical parameters. These diminutive nanoparticles are promising antimicrobial agents and evince a great potential in medical applications.

**INTRODUCTION:** Nanotechnology is a propitious sector of research in modern materials science. Most of the physical and chemical methods of nanoparticle synthesis can control the size and shape of nanoparticles. But these techniques use toxic chemicals in the synthesis thus causing contamination, employ toxic solvents, and generate hazardous by-products.

Green synthesis scores better than chemical and physical method as it is cost effective, eco-friendly, easily scaled up for large-scale synthesis and it is not necessary to employ high energy, temperature, pressure, and toxic chemicals. Employing plants for nanoparticle synthesis is preferable over other biological processes as they are easily available, safe to handle, it eliminates the elaborate process of maintaining cell cultures, and possess a broad variability of metabolites that act as reducing agents.

Silver manifests a powerful inhibitory and a broad spectrum of antimicrobial activity, which was handed down from the past to check and nurse

<p><b>QUICK RESPONSE CODE</b></p> 	<p><b>DOI:</b> 10.13040/IJPSR.0975-8232.8(10).4261-72</p>
<p>Article can be accessed online on: <a href="http://www.ijpsr.com">www.ijpsr.com</a></p>	
<p>DOI link: <a href="http://dx.doi.org/10.13040/IJPSR.0975-8232.8(10).4261-72">http://dx.doi.org/10.13040/IJPSR.0975-8232.8(10).4261-72</a></p>	

diverse infections and diseases<sup>1</sup>. The discovery of antibiotics, lead to the decline in the utilization of silver. Recurrent and blind use of antibiotics posed a consequential and a grave problem of resistance emergence in disease provoking microorganisms to varied antibiotics. Resistance to antibiotics is a deep cause of concern in the medical discipline. To eliminate this problem of resistance, research has set its eyes on the use of silver, by transforming the bulk silver from silver salts like AgNO<sub>3</sub> and AgCl into nanoform, *i.e.* silver nanoparticles.

Metal nanoparticles possess characteristic physical, electronic, electrical, chemical, magnetic, mechanical, dielectric, thermal, optical and biological properties since they harbour exorbitant surface-to-volume ratio, surface energy, spatial confinement and minimized imperfections, in contrast to bulk materials<sup>2,3</sup>. These multidisciplinary properties of nanoparticles have unearthed substantial applications in optoelectronics<sup>4</sup>, information storage<sup>5</sup>, sensor technology<sup>6</sup>, water treatment<sup>7</sup>, cosmetology<sup>8</sup>, textile industry<sup>8,9</sup>, food packaging industry<sup>8</sup>, anti-inflammatory<sup>10</sup>, anti-platelet activities<sup>11</sup>, antifungal<sup>12</sup>, biological labelling<sup>5</sup>, drug delivery<sup>13</sup>, implantable biomaterial<sup>14</sup>, molecular imaging<sup>15</sup>, wound healing<sup>17</sup> and as excellent catalysts<sup>17</sup>. Amidst the other counter-parts, silver nanoparticles are prospective nano-material due to their distinctive physicochemical and antimicrobial properties<sup>18</sup>.

The potential of plant extracts in the reduction of metal ions in the early 1900's was familiar, but the inherent attribute of reducing agents employed was not well understood. The utility of live plants or whole plant extract and plant tissue for reducing metal salts to nanoparticles has captured the attention of researchers within the past 30-years<sup>19</sup>. A thorough literature survey reveals that various plants such as *Nelumbo nucifera* (seed)<sup>20</sup>, Bamboo (leaves)<sup>21</sup>, *Nitraria schoberi* (fruits)<sup>22</sup>, *Loquat* (leaf)<sup>23</sup>, *Carob* (leaf)<sup>24</sup>, *Silybum marianum* (seed)<sup>25</sup>, *Malus domestica* (fruit)<sup>26</sup>, *Myristica fragrans* (seed)<sup>27</sup>, *Vitis vinifera* (leaves and seeds)<sup>28</sup>, Orange peel<sup>29</sup>, *Azadirachta indica* (leaf)<sup>30</sup> etc. were used in the fabrication of nanoparticles.

For the present study we used *Petrea volubilis* L. leaf broth to fabricate eco-friendly silver nanoparticles. Various sizes of silver nanoparticles were

synthesized by employing physico-chemical parameters such as contact time, leaf broth quantity, pH, temperature, and silver nitrate concentration. No hazardous chemicals were used in the reduction of silver ions. Thus synthesized AgNPs were subjected to characterization. a) The visual observation *i.e.* change in the colour of the reaction mixture from pale yellow to dark brown colour stipulated the formation of AgNPs and this observation was confirmed by the SPR bands developed by UV-vis spectroscopy. b) FTIR spectroscopy analysis was executed to ascertain the phytochemicals present in the *Petrea volubilis* L. leaf broth that were accountable for the reduction and capping of silver ions. c) Zeta potential measurements and XRD patterns illustrated that the capping molecules were negatively charged and the NPs were passably stable and crystalline. d) Energy-Dispersive X-ray Spectroscopy (EDS) sensed the presence of elemental silver in the reaction mixture. e) The morphology and sizes of the synthesized nanoparticles were analysed by HRTEM analysis. f) Thus synthesized AgNPs were evaluated for antimicrobial activity which exhibited appealing results.

## MATERIALS AND METHODS:

**Materials:** Silver nitrate (AgNO<sub>3</sub>) was purchased from Sigma-Aldrich chemicals and was used as received. The glass wares were washed with dilute nitric acid and milli-Q water and then dried in hot air oven. Silver nanoparticles were synthesized using *Petrea volubilis* leaf broth. Healthy leaves of *Petrea volubilis* were collected from the Karnatak University campus, Dharwad, Karnataka, India (2015). The leaves were thoroughly washed with milli-Q water to eliminate any surface contamination. About 5gm of the clean leaves were incised.

They were boiled in 100ml milli-Q water for 10 minutes on water bath at 50 °C. The resulting extract was cooled to room temperature and filtered with whatman no.1 filter paper to obtain the filtrate. The filtrate was collected in a 250ml Erlenmeyer flask and stored in the refrigerator at 4 °C to be used within a week. This filtrate was later used for the preparation of silver nanoparticles. 1mM AgNO<sub>3</sub> solution was prepared by dissolving 0.1699 grams silver nitrate (AR grade) in 1liter milli-Q water.

Typical reaction mixture contained 5mL of the leaf broth in 95mL of  $1 \times 10^{-3}$  m aqueous  $\text{AgNO}_3$  solution. The different physico-chemical parameters used in this work were contact time (1, 2, 4, 6, 24, 48, 72 hrs), the leaf extract quantity (5.0, 6.0, 7.0 and 8.0ml), the pH (pH 5, 6 and 7), the temperature (20 °C, 30 °C, 40 °C and 50 °C and the silver salt concentrations (1.0, 1.50 and 2.0 mM). The reduction process in the reaction mixture resulted in change in colour of the solution from pale yellow to dark brown depending on different physico-chemical parameters under investigation.

**Characterization:** UV-vis spectral analysis was performed on Jasco V-670 UV-vis NIR spectrophotometer operated at a resolution of 1nm at room temperature. The FTIR spectra of silver nanoparticles samples were recorded at room temperature with U-3010 spectrophotometer in the region of  $500\text{-}4000\text{cm}^{-1}$  at a resolution of  $4\text{ cm}^{-1}$ . A small quantity of the synthesized silver nanoparticles sample (0.5–3mg) was dried and mixed with 25mg of KBr to form a pellet, which was used for FTIR measurements. XRD analyses were performed. Silver nanoparticles were dispersed in 10ml of milli-Q water and freeze dried. The dried mixture of silver nanoparticles was analysed by an X'Pert Pro X-ray diffractometer operated at a voltage of 40 kV and a current of 30mA with  $\text{Cu K}\alpha$  radiation in  $2\theta$  configurations.

Zeta potential of colloidal solution of nanoparticle was subjected to data acquisition using Zetasizer (Nano ZS) Instrument (Malvern instrument). The purity of the AgNPs were analyzed in a range 2-4 keV by Energy-dispersive X-ray spectroscopy (FEI Quanta FEG 200). The surface morphology, size and diffraction of the AgNPs were measured at different magnification at 100 keV using JEOL 3010 HRTEM.

#### Anti-microbial Assay:

**Anti-bacterial Activity:** Peptone - 10g, NaCl - 10g and Yeast extract 5g, Agar 20g in 1000ml of distilled water. At first stock cultures of bacteria *Staphylococcus aureus* MTCC3160 (gram positive bacteria), *Salmonella typhi* MTCC3216 (gram negative bacteria), was inoculated to the broth media and grown at 37 °C for 18 hrs. Later wells were made in the agar plates. Then 18hr old cultures (100 $\mu$ l, 10-4 cfu) were inoculated and

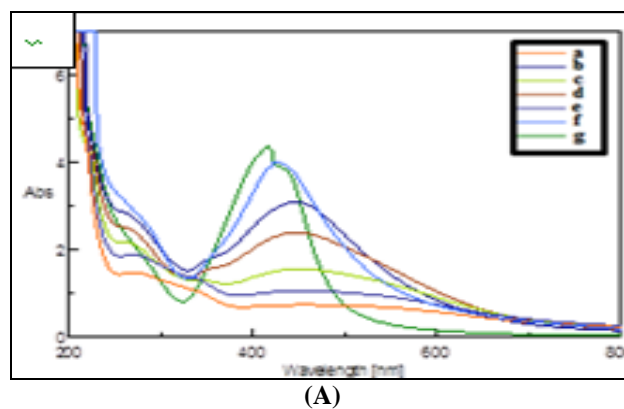
spread evenly on the plate. Well diffusion method was used in the experiments. After 20 min the samples (20, 40, 60, 80, 100 $\mu$ l) were filled in the wells. All the plates were incubated at 37 °C for 24 hr. The diameter of inhibition zone were measured in mm. Standard agar well diffusion method was carried out against the test bacterial species.

**Anti-fungal Activity:** Czapek-Dox Agar: Composition (g/l) Sucrose-30.0; Sodium nitrate-2.0;  $\text{K}_2\text{HPO}_4$ -1.0,  $\text{MgSO}_4 \cdot 7\text{H}_2\text{O}$ -0.5; KCl-0.5;  $\text{FeSO}_4$ -0.01; Agar-20; Initially, the stock culture of the fungi *Aspergillus flavus* MTCC1883 was inoculated in the broth media and allowed to grow at 27 °C for 48 hrs. The 48 hr old cultures (100 $\mu$ l 10<sup>4</sup> CFU) were inoculated in each plate and spread evenly. Well diffusion method was used in the experiments.

The wells were made in the agar plates. After 20 min the test compound (20, 40, 60, 80, 100 $\mu$ l) were filled in the wells at different concentrations. All the plates were incubated at 27 °C for 96 hr and the diameter of inhibition zone was measured in mm. Standard agar well diffusion method was carried out against the test fungi.

## RESULTS AND DISCUSSION:

**Effect of Contact Time on the Phyto-synthesis of AgNPs:** The effect of contact time (1, 2, 4, 6, 24, 48 and 72 hrs) was investigated on the biogenically synthesised of silver nanoparticles (**Fig. 1a**). The other reaction conditions include leaf extract quantity 5ml, pH 7, temperature 35 °C and silver nitrate concentration of 1mM. Nanoparticle formation was initiated within 15 min. This was confirmed with increase in colour intensity of the reaction mixture, *i.e.* from pale yellow to dark brown as the time duration increased.





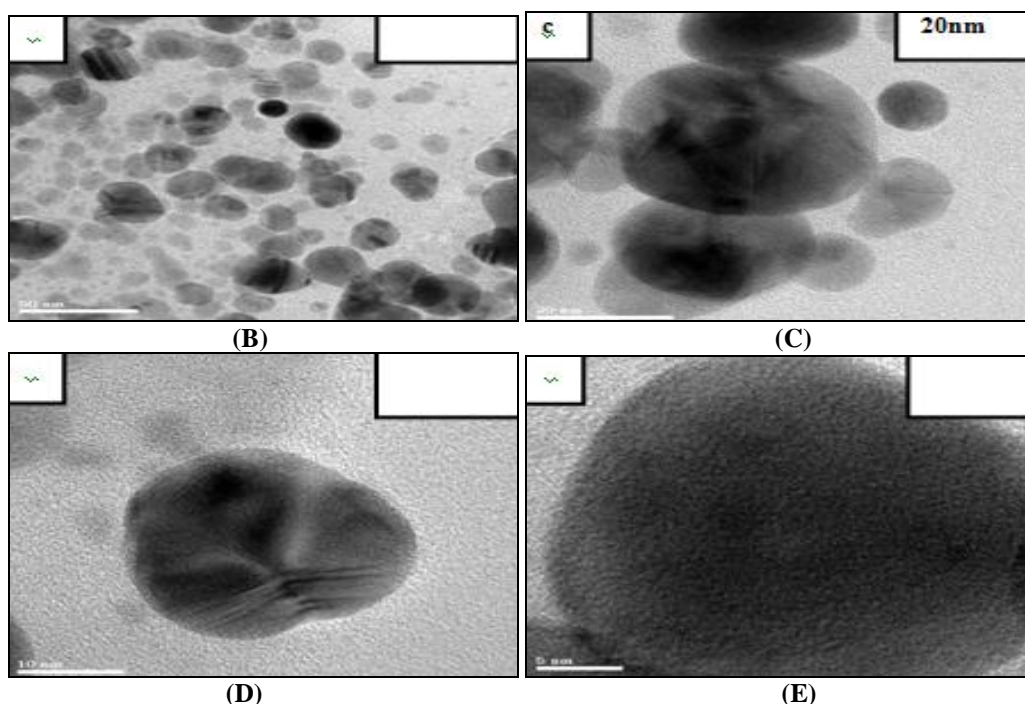


**FIG. 1:** A) UV-VIS ABSORPTION SPECTRA OF AgNPs AT DIFFERENT CONTACT TIME. [a- 1 hr, b-2 hrs, c-4hrs, d-6 hrs, e-24 hrs, f-48 hrs AND g-72 hrs]. HRTEM IMAGES OF AgNPs AT DIFFERENT CONTACT TIME B) AND C) 1 hrs AND 24 hrs - 50nm AND 20 nm D) 48 hrs -10 nm AND E) 72 hrs -5nm

This change in colour of the reaction mixture is attributed to the excitation of surface plasmon vibrations in Ag nanoparticles. The data shows a red shift in the peak wave length at 456nm at 1 hr which increases steadily in intensity and reaches stabilization at 415nm at 72 hrs in the blue shift region (Fig. 1a). The absorption peak reflects the size and shape of the nanoparticles. The broadening of absorption spectra at lower contact time duration was due to the formation of large sized nanoparticles. As the incubation time accelerates further, intense peaks were observed indicating the

synthesis of small sized nanoparticles<sup>31</sup>. This was confirmed by HRTEM microphotographs, where the sizes of nanoparticles range between 50 to 20nm at 1, 2, 4, 6 and 24 hrs (Fig. 1b and c), 20-10nm at 48 hrs (Fig. 1d) and 10-5nm at 72 hrs (Fig. 1e) respectively. Zeta potential values show -19.7, -19.9, -20.6, -21.5, -22.7, -23.1 and -23.2 at 1, 2, 4, 6, 24, 48 and 72 hrs of contact time. The zeta potential data suggests that the capping molecules are negatively charged and the synthesized nanoparticles are moderately stable.

#### Effect of Leaf Broth Quantity on the Phyto-Synthesis of AgNPs:

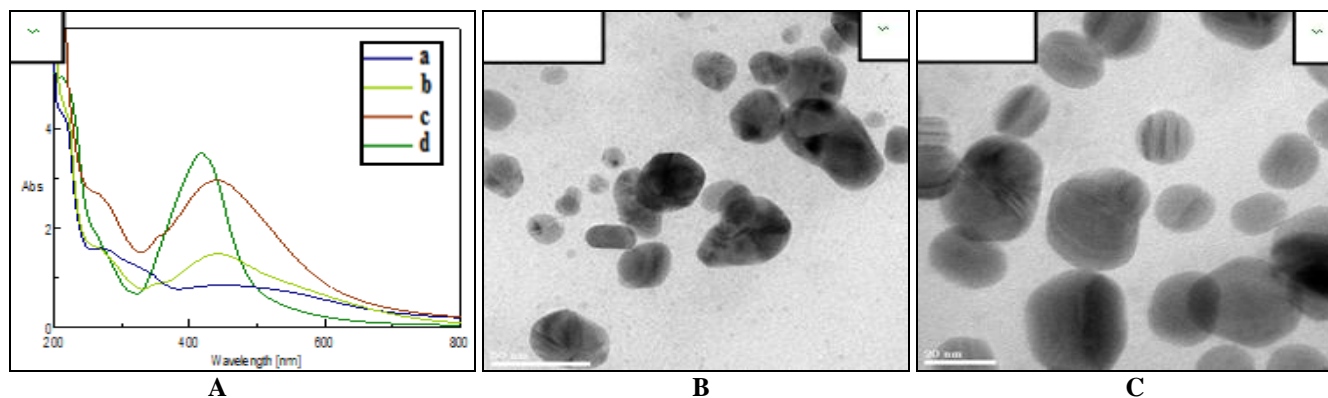


**FIG. 2:** A) UV-VIS ABSORPTION SPECTRA OF AgNPs AT DIFFERENT LEAF BROTH QUANTITY. [a- 5ml, b-6ml, c-7ml AND d-8ml]. HRTEM IMAGES OF AgNPs AT DIFFERENT LEAF sBROTH QUANTITY. B) 5ml, 6ml AND 7ml -50nm C) 8ml - 20nm

Different leaf broth quantity was used (5, 6, 7, and 8 ml). The other reaction conditions include contact time 24 hrs, pH 7, temperature 35 °C and silver nitrate concentration of 1mM. There was change in the colour of the reaction mixture with increase in the quantity of the leaf broth. The colour of the reaction mixture gradually turned deep brown with increase in leaf broth quantity. The UV-vis data shows 450, 442, 440 and 418 nm at 5, 6, 7, and 8ml of the leaf broth quantity (**Fig. 2a**). This decrease in absorbance indicates a reduction in the mean diameter of the nanoparticles. Based on the UV-vis spectra the sharpness of the absorption peak relies on the quantity of leaf broth, thus being more intense with a higher quantity of leaf broth. The above results are in accordance with the results of the experiments conducted with bark extract of *Cinnamomum zeylanicum* and with the leaves of

*Cinnamomum camphora*<sup>32, 33</sup>. According to HRTEM microphotographs the size of nanoparticles range between 50-30nm at 5, 6 and 7ml (**Fig. 2b**) and 20nm at 8ml (**Fig. 2c**) of leaf extract quantity. It was also observed that the nanoparticles formed were spherical in shape. The Zeta potential analysis shows -20.0, -20.6, -21.0 and -21.2, at 5, 6, 7 and 8ml of leaf broth quantity. The negative values indicate that the capping molecules on AgNPs were negatively charged and the nanoparticles were moderately stable. With increase in leaf broth quantity there was decrease in the particle size due to the availability of more reducing bio-molecules for the reduction and capping of silver ions and protecting them from aggregation. A similar effect was observed with increase in *Magnolia kobus* leaf extract<sup>34</sup>.

### Effect of pH on the Phyto-synthesis of AgNPs:

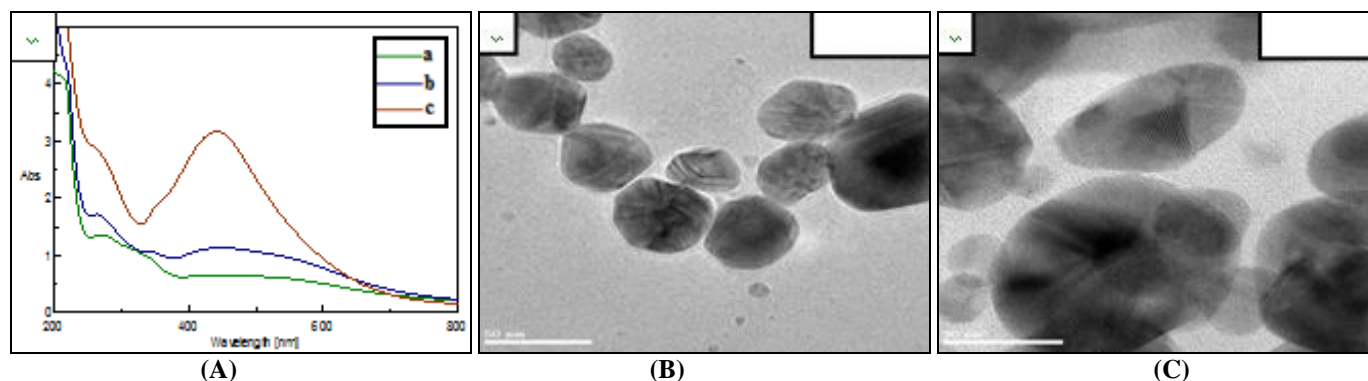


**FIG. 3: A) UV-VIS ABSORPTION SPECTRA OF AgNPs AT DIFFERENT pH [a-pH 5, b-pH 6 AND c-pH 7]. HRTEM IMAGES OF AgNPs AT DIFFERENT pH B) pH 5 AND pH 6 – 50nm C) pH 7- 20nm**

Experiments were performed by varying the pH (pH 5, 6 and 7) of the reaction mixture to study the effect of pH on the synthesis of silver nanoparticles (**Fig. 3a**). The other reaction conditions include contact time 24 hrs, leaf extract quantity 5ml, temperature 35 °C and silver nitrate concentration of 1mM. It was observed that with the gradual change in pH, the color of the reaction mixture changed from light yellow to dark brown due to excitation of surface plasmon resonance (SPR) of the AgNPs, which confirms the synthesis of silver nanoparticles. The outcomes of UV-vis spectra revealed 451nm, 448nm and 442nm at pH 5, 6 and 7 (**Fig. 3a**). With the rise in pH the absorption peaks became more intense and shift to shorter wavelength due to decrease in the size of the biogenically synthesized silver nanoparticles<sup>35-37</sup>.

HRTEM microphotograph revealed the size of the nanoparticles in the range 50-20nm at pH 5 and 6 (**Fig. 3b**) and 20nm at pH 7 (**Fig. 3c**). It was observed that the particle size is larger in acidic medium and smaller in basic medium. The zeta potential data shows -20.6, -21.4 and -22.0 at pH 5, 6 and 7 indicating that the capping molecules are negatively charged and are stable. It is observed that acidic condition suppresses while the basic condition accelerates the formation of silver nanoparticles. This is because extremely acidic conditions render the biomolecules present in the plant extract to be inactive<sup>38</sup>. The aggregation of silver nanoparticles to form large nanoparticles at low pH (pH 5), is favoured over the nucleation. Since a large number of functional groups are available for silver binding at elevated pH, large

number of nanoparticles with smaller diameters are synthesised. Moreover at elevated pH more spherical shaped nanoparticles were formed rather than ellipsoidal nanoparticles. The investigation reveals that the pH played an important role in

controlling the size of the silver nanoparticles. A similar pH effect was reported at elevated pH in addition to the complete and rapid reduction of the silver nanoparticles<sup>39</sup>.

#### Effect of Temperature on the Phyto-synthesis of AgNPs:

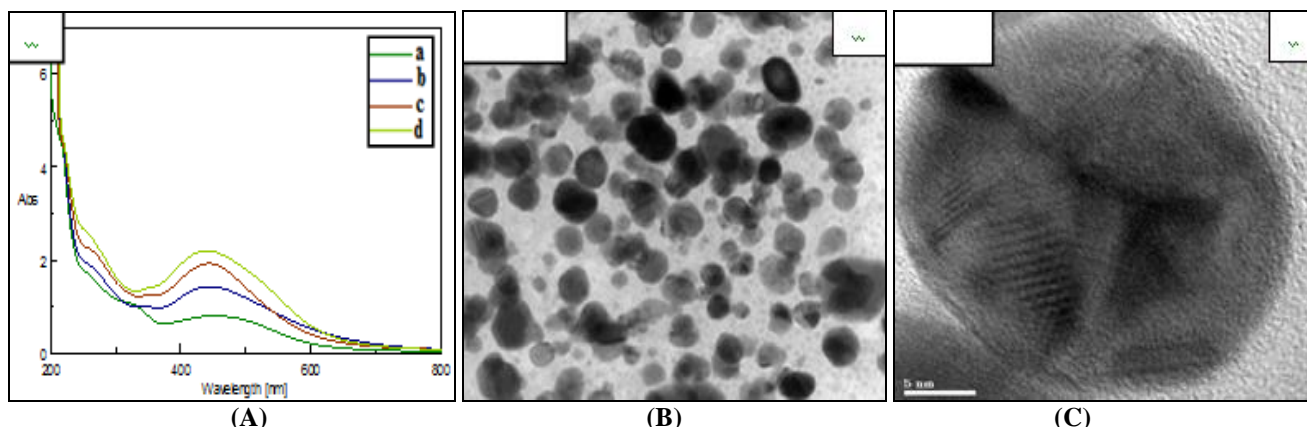


**FIG. 4: A) UV-VIS ABSORPTION SPECTRA OF AgNPs AT DIFFERENT INCUBATION TEMPERATURE. [a-20 °C, b-30 °C, c-40 °C AND d-50 °C]. HRTEM IMAGES OF AgNPs AT DIFFERENT INCUBATION TEMPERATURE. B) 20 °C-50nm C) 50 °C – 5nm**

The temperature of the reaction mixture was varied (20, 30, 40 and 50 °C). The other reaction conditions include contact time 24 hrs, leaf extract quantity 5ml, pH 7, and silver nitrate concentration of 1mM. The UV-vis absorption peaks occurred at 452, 445, 444 and 440nm at 20, 30, 40 and 50 °C (**Fig. 4a**). As the reaction temperature increased from 20 °C to 50 °C, the SPR bands became sharper and shifted to shorter wavelengths. This shift indicated the decrease in the particle size. HRTEM analysis showed that the nanoparticles range in size between 50-5nm at 20, 30, 40 and 50 °C (**Fig. 4b** and **4c**). As shown in the HRTEM microphotograph, all the particles were almost spherical nanoparticles. Zeta potential values show -20.6, -21.4, -23.6, and -24.9 from 20 °C to 50 °C of temperature. This indicates that the capping molecules are negatively charged and the nanoparticles are stable. The nanoparticle synthesis is affected by the temperature in various ways. For instance, when the fungus *Trichoderma viride* was used in the synthesis of biogenic silver nanoparticles, the size of nanoparticles decreased with an increase in temperature<sup>40</sup>. This results due to the reactants in the reaction mixture being consumed rapidly with the rise in temperature and eventually leading to the formation of smaller sized nanoparticles.

At higher temperatures the silver ions could be consumed mainly on the formation of nuclei, while the secondary reduction process is hindered which takes place on the surface of the preformed nuclei. Therefore with increase in temperature the nanoparticle size decreases<sup>38</sup>.

**Effect of Silver Nitrate Concentration on the Phyto-synthesis of AgNPs:** A variation in the biological material and metal salt concentration influences nanoparticle synthesis<sup>41</sup>. The reaction conditions include contact time 24 hrs, leaf extract quantity 5ml, pH 7, and temperature 35 °C. The silver nitrate concentration was varied (1.0, 1.50 and 2.0 mM). The absorption spectra shows peak at 442, 449 and 454 nm (**Fig. 5a**). Peak absorbance increases and shifts to higher wavelengths at higher silver nitrate concentration. At lower silver nitrate concentration (1mM) the absorption peak decreases in band width and increases in band intensity which indicates the formation of smaller and spherical shaped particles. HRTEM microphotographs show different sizes that range from 5-50 nm at 1.0, 1.50 and 2.0mM of silver salt concentration (**Fig. 5b** and **5c**). The zeta potential values show -23.5, -22.9 and -22.8 at 1.0, 1.50 and 2.0mM of silver salt concentration. This shows that the capping molecules are negatively charged, and the

nanoparticles are moderately stable. Increase in the concentration of the metal ion, results in increase in nanoparticle size which was confirmed from HRTEM images. This could be due to the secondary reduction process that takes place due to the absorption of too many silver ions on the surface of preformed nuclei, leading to formation

of larger nanoparticles<sup>38</sup>. In case of silver nanoparticles, the absorbance peak broadens with increase in metal ion concentration indicating synthesis of large sized nanoparticles. Similar results are obtained using the seed extract of *Jatropha curcas* with different concentrations of silver nitrate<sup>42</sup>.

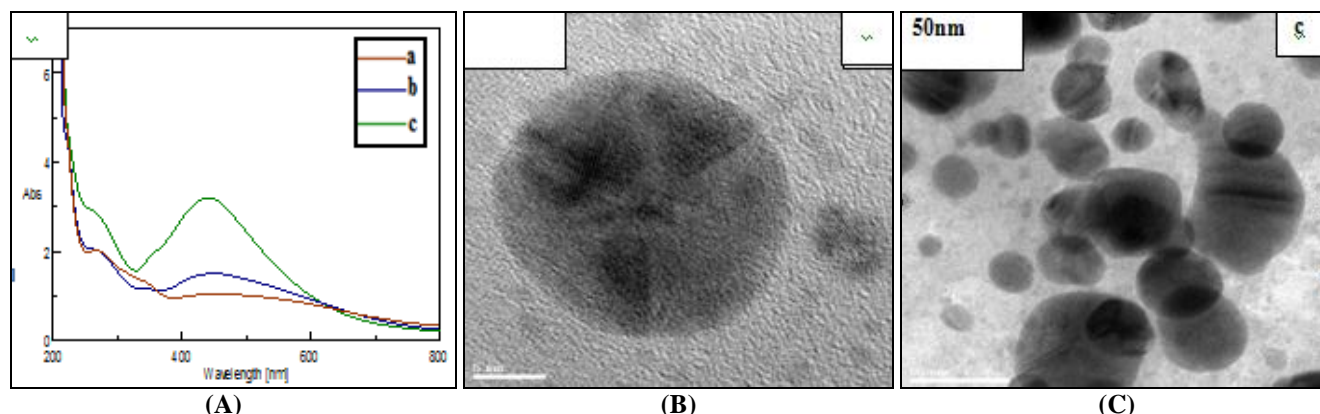


**FIG. 5: A) UV-VIS ABSORPTION SPECTRA OF AgNPs AT DIFFERENT SILVER NITRATE CONCENTRATION. [a-1.0mm, b-.50mm AND c-2.0MM], HRTEM IMAGES OF AgNPs AT DIFFERENT SILVER NITRATE CONCENTRATION. B) 1.0mm - 5 nm, AND C) 1.50 AND 2.0mm - 50nm**

**Fourier Transform Infrared Spectroscopy (FTIR):** FT-IR spectroscopy analysis was carried out to investigate the possible biomolecules that brought about the reduction, capping and stabilization of the Ag nanoparticles. The band intensities of infrared spectra of silver nanoparticles synthesized using *P. volubilis* leaf are depicted in (Fig. 6 and Table 1). The spectra showed shift in the strong absorption peaks at  $3422.30\text{cm}^{-1}$  -  $3376.10\text{cm}^{-1}$ ,  $2923.76\text{cm}^{-1}$  -  $2916.76\text{cm}^{-1}$ ,  $2854.13\text{cm}^{-1}$  -  $2852.00\text{cm}^{-1}$ ,  $1748.16\text{cm}^{-1}$  -  $1739.33\text{cm}^{-1}$ ,  $1639.37\text{cm}^{-1}$  -  $1616.09\text{cm}^{-1}$ ,  $1109.40\text{cm}^{-1}$  -  $1076.49\text{cm}^{-1}$  (Fig. 6 and Table 1). A large shift in the absorbance peak with low band intensity was observed from  $3422.30\text{cm}^{-1}$  to  $3376.10\text{cm}^{-1}$  and  $1109.40\text{cm}^{-1}$  -  $1076.49\text{cm}^{-1}$ , corresponds to O-H stretching due to carboxylic acids and C-N

stretching of aliphatic amines or C-O stretching vibrations of phenolic compounds implying the binding of silver ions. The peak at  $2923.76\text{cm}^{-1}$  -  $2916.76\text{cm}^{-1}$  and  $2854.13\text{cm}^{-1}$  -  $2852.00\text{cm}^{-1}$ , is attributed to the aldehydic CH stretching and asymmetric stretching of the  $\text{CH}_3$  group. The shift in absorption peak at  $1748.16\text{cm}^{-1}$  -  $1739.33\text{cm}^{-1}$  is due to C=O stretching mode of the carbonyl functional groups which brings about reduction of silver ions to silver nanoparticles. (C=O) $\text{NH}_2$  group present in the secondary metabolites of the leaf broth brings about shift in the absorption band ( $1639.37\text{cm}^{-1}$  -  $1616.09\text{cm}^{-1}$ ). The shifting of the weak band  $1109.40\text{cm}^{-1}$  -  $1076.49\text{cm}^{-1}$  is due to the presence of C-N stretching of aliphatic amines or C-O stretching vibrations of phenolic compounds.

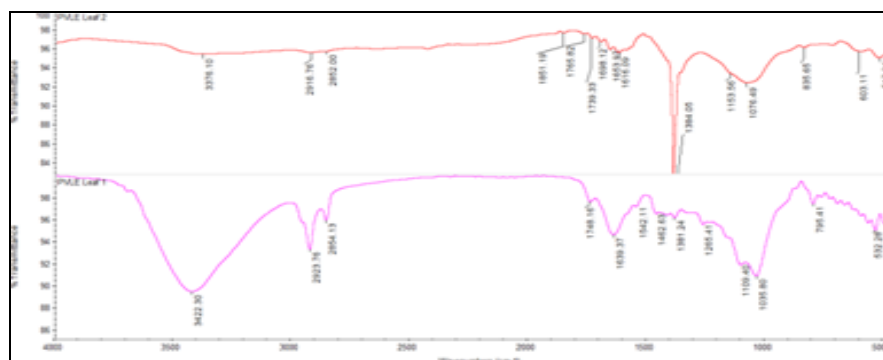


**FIG. 6: FTIR SPECTRA OF PETREA VOLUBILIS LEAF BROTH AND SILVER NANOPARTICLES SOLN**



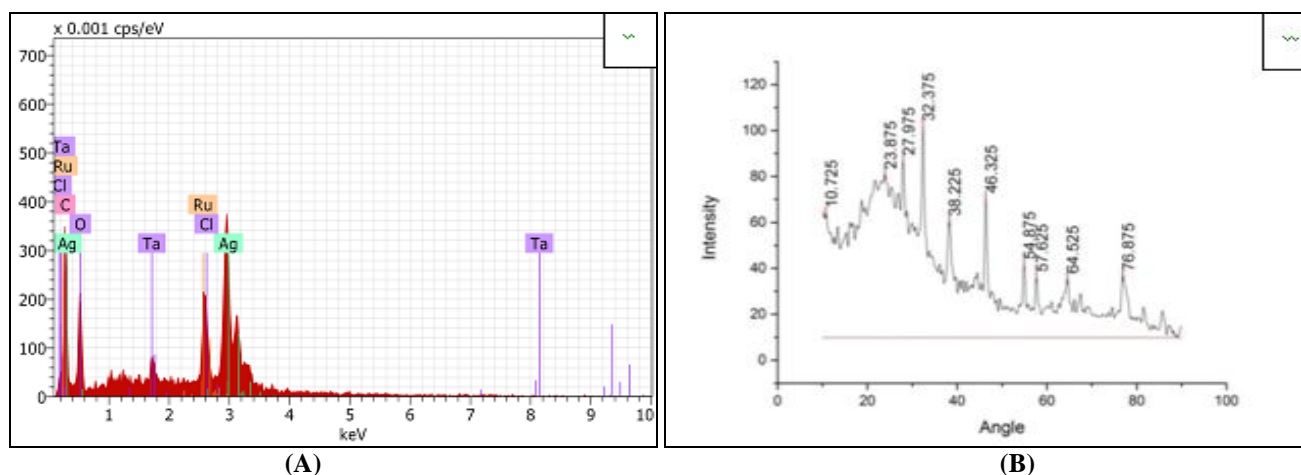
**TABLE 1: FTIR MEASUREMENTS OF THE *PETREA VOLUBILIS* LEAF BROTH AND SILVER NANOPARTICLES SYNTHESIZED**

Sl. no	Absorption peak $\text{cm}^{-1}$ or leaf broth	Absorption peak $\text{cm}^{-1}$ of Silver nanoparticles	Functional groups
1	3422.30	3376.10	O-H stretching
2	2923.76	2916.76	Aldehydic CH stretching
3	2854.13	2852.00	Asymmetric stretching of the $\text{CH}_3$ group
4	1748.16	1739.33	C=O stretching
5	1639.37	1616.09	(C=O) $\text{NH}_2$ group
6	1109.40	1076.49	C-N or C-O stretching vibration

The reports indicate that carboxylic acids and aldehydic CH stretching,  $\text{CH}_3$  group, carbonyl functional groups, C–N stretching of aliphatic amines or C–O stretching vibrations of phenolic compounds were responsible for the reduction of silver ions to silver nanoparticles.

**Energy Dispersive X-ray Analysis (EDS):** The energy in keV is on the horizontal axis while the X-ray counts are shown in the vertical axis. EDS analysis shows the presence of elemental silver, which is depicted in the graph (**Fig. 7a**).

In *P. volubilis* leaf the energy peaks of 2–4 keV are reported for silver atoms. The other biomolecules capping the nanoparticles are tantalum, ruthenium, chloride and oxygen. The C signal seen in the graph may be due to X-ray emission from the biomolecules present in the *P. volubilis* leaf broth (**Fig. 7a**). The major emission energy at 3keV depicts that the silver is accurately identified. In a previous study formation of silver nanoparticles in the range 2.5–4keV by using *Alfalpa* was reported<sup>43</sup>.

**FIG. 7: A) EDX OF BIOGENIC SILVER NANOPARTICLES. B) XRD PATTERN OF THE BIOSYNTHESIZED SILVER NANOPARTICLES**

**X-ray Diffraction (XRD):** XRD analysis of the biosynthesized silver nanoparticles (**Fig. 7b**) was performed. XRD report obtained for synthesized silver nanoparticles shows a characteristic high intensity peak at  $2\theta = 76.88^\circ$  (**Fig. 7b**). This corresponds to pure silver showing Bragg reflections of (311) set of lattice plane, which is well co-ordinated with the existing Joint Committee on Powder Diffraction Standards (JCPDS File No. 04-0783). The peaks at  $2\theta$  values of 32.38, 38.23, 46.33, 54.88, 57.63, 64.53 and 76.88 can be indexed as (111), (111), (200), (200), (200), (220), (311) planes of fcc silver (**Fig. 7b**).

An XRD spectrum compared with the standard confirmed that the silver nanoparticles are crystalline in nature. The average nanocrystalline size was calculated by using Debye–Scherrer formula,

$$D = k\lambda / \beta \cos\theta$$

Where D is particle diameter size,  $\lambda$  is wavelength of X-ray source (0.1541 nm), k is a constant equals 1,  $\beta$  is the full width at half maximum (FWHM) and  $\theta$  is the diffraction angle. The average size of the crystallite according to Debye–Scherrer equation is found to be 21nm. The XRD patterns



obtained in the study confirms with the earlier reports<sup>42, 32</sup>.

**Antimicrobial Efficacy:** The metal nanoparticles show effective anti-microbial activity<sup>44</sup>. High anti-microbial activity of AgNPs is due to their small size<sup>45</sup> and their large surface area. The outcomes of the anti-bacterial and anti-fungal activity are shown in (Fig. 8). The highest anti-bacterial activity was observed against *S. aureus* whose ZOI diameter was 15mm at 100 $\mu$ l (Fig. 8D). *S. typhi* showed a ZOI diameter of 14mm at 100 $\mu$ l (Fig. 8E). The highest antifungal activity by *P. volubilis* leaf was observed against *A. flavus* whose ZOI diameter is 8mm at 100 $\mu$ l (Fig. 8F). The fabricated nanoparticles shows good bactericidal activity compared to the test fungi. The *P. volubilis* leaf broth did not show any zone of inhibition. (Fig. 8a, b and c). These results are in accordance with the work carried out previously<sup>46-48</sup>.

The precise mechanism of the microbicidal effect of silver nanoparticles is not very well understood. However three types of antibacterial mechanisms were observed<sup>49</sup>, i.e. (i) Plasmolysis, the separation

of the cytoplasm of the bacterial cell from bacterial cell wall, were observed in Gram +ve bacteria and Gram -ve bacteria, (ii) inhibition of the cell wall synthesis and (iii) induces metabolic disturbances in the pathogenic bacteria. Reports on the mechanism of anti-fungal action of silver ions on fungi have shown that, DNA loses its potential to replicate resulting in the inactivation of ribosomal subunit proteins<sup>50, 51</sup>.

Certain other cellular proteins and enzymes essential for ATP production also become inactive. It has also been stated that the functioning of membrane-bound enzymes, such as those in the respiratory chain have primarily been affected by the silver ions. In SEM study with *C. albicans* and *Saccharomyces cerevisiae* cells, the interaction between silver nanoparticles and their membrane structure show the formation of "pits" on their surfaces, which results in the formation of pores. This causes the leakage of ions and other materials, dissipating the electrical potential of the membrane and finally resulting in the death of the cell.

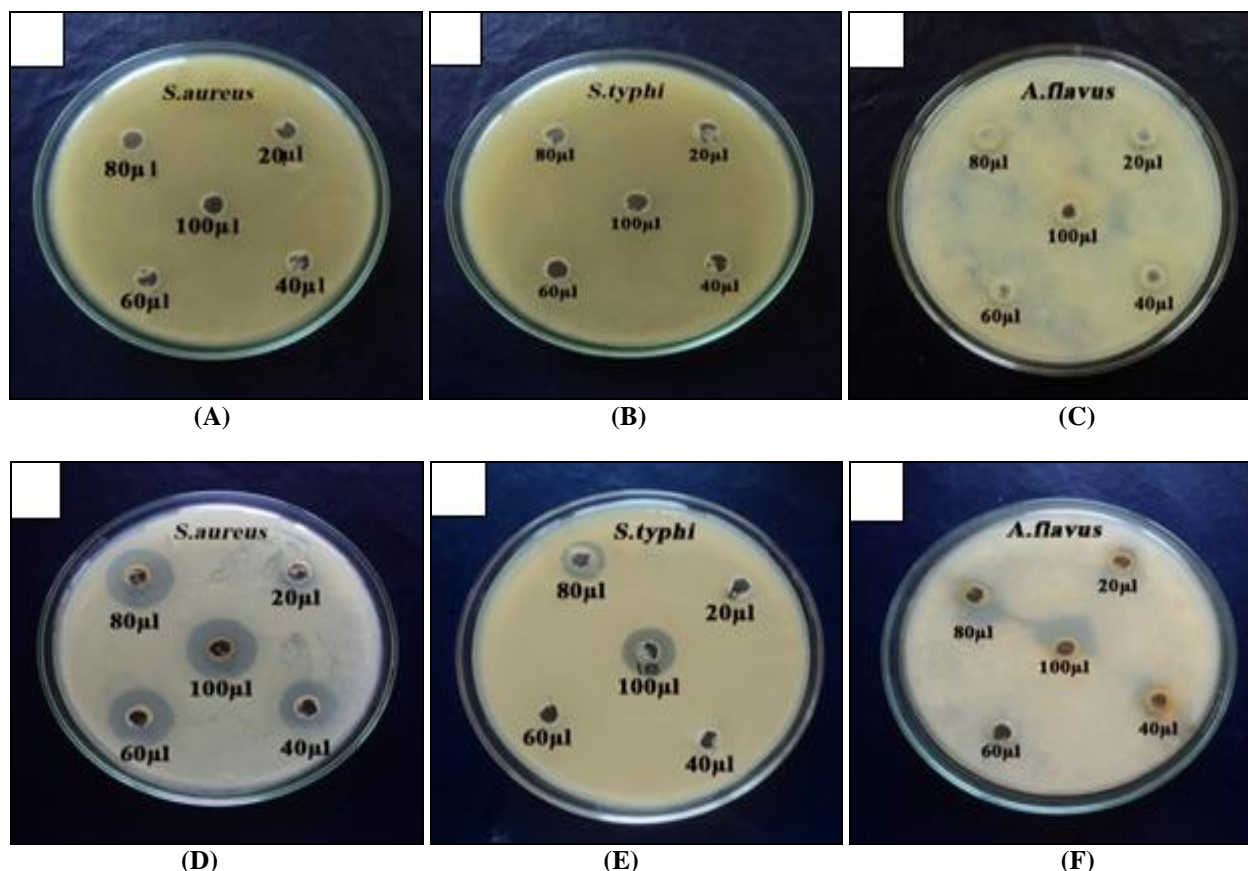


FIG. 8: A) B) & C) *S. AUREUS*, *S. TYPHI* & *A. FLAVUS* WITH LEAF EXTRACT – NO ZONE OF INHIBITION, D) *S. AUREUS* WITH ZOI - 40 $\mu$ l-9mm, 60 $\mu$ l-12mm, 80 $\mu$ l-13mm, 100 $\mu$ l-15mm. E) *S. TYPHI* WITH ZOI - 80 $\mu$ l-7mm, 100 $\mu$ l-14mm. F) *A. FLAVUS* WITH ZOI - 80 $\mu$ l-5mm and 100 $\mu$ l-8mm

**CONCLUSION:** Phytosynthesis of silver nanoparticles and their anti-microbial activity using leaf broth of *P.volubilis* were studied. The physico-chemical parameters were observed to play a crucial role in the fabrication of nanoparticles of various sizes. According to UV-vis spectroscopy analysis the narrowing of the absorption peaks was observed and HRTEM observations showed decrease in the nanoparticle size with increase in contact time, quantity of leaf broth, pH and temperature. But broad absorption peak was seen in UV-vis data and HRTEM results which showed increase in the nanoparticle size with increase in silver nitrate concentration. Zeta potential data showed that the capping molecules were negatively charged and the nanoparticles were stable.

FTIR analysis shows that the carboxylic acids and aldehyde CH stretching, CH<sub>3</sub> group, carbonyl functional groups, C–N stretching of aliphatic amines or C–O stretching vibrations of phenolic compounds were responsible for the bio reduction and capping of silver ions. EDS and XRD results confirms the presence of the elemental silver in the reaction mixture, as depicted in the graph and also indicates the crystalline nature of the nanoparticles.

The highest anti-bacterial activity was observed against the gram +ve bacteria, *S. aureus* whose ZOI was 15mm at 100µl compared to *S. typhi* a gram -ve bacteria whose ZOI was 14mm at 100µl. The antifungal activity was observed against *A. flavus* whose ZOI showed 8mm at 100µl.

The present investigation demonstrates a rapid, eco-friendly, cost efficient and a simple method for the fabrication of silver nanoparticles of different sizes and inhibitory activity against the microbes.

**ACKNOWLEDGEMENTS:** The authors thank the chairman, Department of botany, Karnatak University, Dharwad. We acknowledge DST unit of Nano science, IIT Madras for HRTEM, SRM University for XRD and ED's measurements and Aimil Malvern for Zeta potential measurements. Authors also thank USIC for instrumentation facility, K. U. Dharwad. One of the authors NIH thanks RFSMS for Junior Research Fellowship and UGC New Delhi for financial support under UGC-SAP-DSA-I phase program of the department.

## REFERENCES:

1. Shankar SS, Rai A, Ahmad A and Sastry M: Rapid synthesis of Au, Ag, and bimetallic Au core–Ag shell nanoparticles using Neem (*Azadirachta indica*) leaf broth. *Journal of Colloid and Interface Science* 2004; 275: 496–502.
2. Schmid G: Large clusters and colloids. *Metals in the embryonic state. Chemical Reviews* 1992; 92: 1709-1727.
3. Daniel MC and Astruc D: Gold nanoparticles: assembly, supra-molecular chemistry quantum- size- related properties, and applications toward biology, catalysis, and nanotechnology. *Chemical Reviews* 2004; 104: 293-346.
4. Gracias DH, Tien J, Breen TL, Hsu C and Whitesides GM: Forming electrical networks in three dimensions by self-assembly *Science* 2000; 289: 1170–1172.
5. Qiu H, Rieger J, Gilbert B, Jerome R and Jerome C: PLA-coated gold nanoparticles for the labeling of PLA biocarriers. *Chemistry of Materials* 2004; 16: 850–856.
6. Gomez-Romero P: Hybrid organic-inorganic materials in search of synergic activity. *Adv. Mater.* 2011; 13: 163–174.
7. Tolaymat TM, Badawy AM, Genaidy A, Scheckel KG, Luxton TP and Suidan M: An evidence-based environmental perspective of manufactured silver nanoparticle in syntheses and applications: a systematic review and critical appraisal of peer-reviewed scientific papers. *Sci. Total Environment* 2010; 408: 999–1006.
8. Pulit J, Banach M and Kowalski Z: Nanosilver - making difficult decisions. *Ecological Chemistry and Engineering* 2011; 18: 185–196.
9. El-Rafie MH, Shaheen TI, Mohamed AA and Hebeish A: Biosynthesis and applications of silver nanoparticles onto cotton fabrics. *Carbohydrate Polymers* 2012; 90: 915–920.
10. Martínez-Gutierrez F, Thi EP, Silverman JM, De Oliveira CC, Svensson SL, Vanden HA, Sánchez EM, Reiner NE, Gaynor EC, Pryzdial EL, Conway EM, Orrantia E, Ruiz F, Av-Gay Y and Bach H: Anti-bacterial activity, inflammatory response, coagulation, and cytotoxicity effects of silver nanoparticles. *Nanomedicine* 2012; 8: 328–336.
11. Ragaseema VM, Unnikrishnan S, Kalliyana KV and Krishnan LK: The antithrombotic and antimicrobial properties of PEG-protected silver nanoparticle-coated surfaces. *Biomaterials* 2012; 33: 3083–3092.
12. Chladek G, Mertas A, Barszczewska - Rybarek I, Nalewajek T, Zmudzki J, Król W and Lukaszczyk J: Antifungal activity of denture soft lining material modified by silver nanoparticles-a pilot study. *International Journal of Molecular Sciences* 2011; 12: 4735–4744.
13. Tom RT, Suryanarayanan V, Reddy PG, Baskaran S and Pradeep T: Ciprofloxacin protected gold nanoparticles. *Langmuir* 2004; 20: 1909–1914.
14. Juan L, Zhimin Z, Anchun M, Lei L and Jinchao Z: Deposition of silver nanoparticles on titanium surface for antibacterial effect. *International Journal of Nanomedicine* 2010; 15: 261–267.
15. Kohl Y, Kaiser C, Bost W, Stracke F, Fournelle M, Wischke C, Thielecke H, Lendlein A, Kratz K and Lemor R: Preparation and biological evaluation of multifunctional PLGA-nanoparticles designed for photoacoustic imaging. *Nanomedicine* 2011; 7: 228–237.
16. Tian J, Wong KK, Ho CM, Lok CN, Yu WY, Che CM, Chiu JF and Tam PK: Topical delivery of silver nanoparticles promotes wound healing. *Chem. Med. Chem* 2007; 2: 129–136.

17. Shiraishi Y and Toshima N: Colloidal silver catalysts for oxidation of ethylene. *Journal of Molecular Catalysis A: Chemical* 1999; 141:187–192.
18. Chen M, Yang Z, Wu H, Pan X, Xie X and Wu C: Antimicrobial activity and the mechanism of silver nanoparticle thermo-sensitive gel. *International Journal of Nanomedicine* 2011; 6: 2873–2877.
19. Mittal AK, Chisti Y and Banerjee UC: Synthesis of metallic nanoparticles using plant extracts. *Biotechnology Advances* 2013; 31: 346–356.
20. Nguyen TMT, Tran NMA, Mai, DT, Thupakula, VMS, Jae-Soon L, Patnamsetty CN and Kap DL: Green Synthesis of Silver Nanoparticles Using *Nelumbo nucifera* Seed Extract and its Antibacterial Activity. *Acta Chim. Slov* 2013; 60: 673–678.
21. Sohail Y, Lin L and Juming Y: Biosynthesis of Silver Nanoparticles by Bamboo Leaves Extract and Their Antimicrobial Activity. *Journal of Fiber Bioengineering and Informatics* 2013; 6: 77-84.
22. Majid SR, Javad SR, Gholam AH, Abdolhossein M and Dhrubo JS: Biological Synthesis of Gold and Silver Nanoparticles by *Nitraria schoberi* Fruits. *American Journal of Advanced Drug Delivery* 2013; 1: 174-179.
23. Awwad AM, Salem NM and Abdeen AO: Biosynthesis of silver nanoparticles using Loquat leaf extract and its antibacterial activity. *Advanced Materials Letters* 2013; 4: 338-342.
24. Awwad AM, Salem NM and Abdeen AO: Green synthesis of silver nanoparticles using carob leaf extract and its antibacterial activity. *International Journal of Infection Control* 2013; 4: 1-6.
25. Mohammad R, Pourseyedi S, Baghizadeh A, Ranjbar S and Mansoori GA: Synthesis of Silver Nanoparticles Using *Silybum marianum* Seed Extract. *International Journal of Nanoscience and Nanotechnology* 2013; 9: 221-226.
26. Umoren SA, Obot IB and Gasem ZM: Green Synthesis and Characterization of Silver Nanoparticles using Red Apple (*Malus domestica*) Fruit Extract at Room Temperature. *Journal of Materials and Environmental Science* 2014; 5: 907-914.
27. Sharma G, Sharma AR, Kurian M, Bhavesh R, Nam JS and Lee SS: Green synthesis of silver nanoparticle using *Myristic afragrans* (nutmeg) seed extract and its biological activity. *Digest Journal of Nanomaterials and Biostructures* 2014; 9: 325–332.
28. Eman HI, Mostafa MHK, Fozia AAS and Fatma El-M: Biosynthesis of Gold Nanoparticles Using Extract of Grape (*Vitis vinifera*) Leaves and Seeds. *PNN* 2014; 3: 1-12.
29. Manal AA, Awatif AH, Khalid MOO, Dalia FAE, Nada EE, Lamia AA, Shorog MA, Nada MM and Abdelalah AGA: Silver nanoparticles biogenic synthesized using an orange peel extract and their use as an anti-bacterial agent. *International Journal of Physical Sciences* 2014; 9: 34-40.
30. Ahmed S, Ahmad M, Swami BL and Ikram S: Green synthesis of silver nanoparticles using *Azadirachta indica* aqueous leaf extract. *Journal of Radiation Research and Applied Sciences* 2015; 9: 1–7.
31. Zhang WZ, Qiao XL and Chen JG: Chem.Synthesis and characterization of silver nanoparticles in AOT micro emulsion system. *Chemical Physics* 2006; 300: 495-500.
32. Kumar SM, Sneha K, Won SW, Cho CW, Kim S and Yun YS: *Cinnamon zeylanicum* bark extract and powder mediated green synthesis of nano-crystalline silver particles and its antibacterial activity. *Colloids and Surfaces B: Bio-interfaces* 2009; 73: 332–338.
33. Huang J, LiQ, SunD, Lu Y, Su Y, Yang X, Wang H, Wang Y, Shao W, He N, Hong J and Chen C: Biosynthesis of silver and gold nanoparticles by novel sundried *Cinnamomum camphora* leaf. *Nanotechnology* 2008; 18: 105104.
34. Song JY and Kim BS: Rapid biological synthesis of silver nanoparticles using plant leaf extracts. *Biotechnology and Bioprocess Engineering* 2009; 32: 79–84.
35. Evanoff DD and Chumanov G: Size-controlled synthesis of nanoparticles. “silver-only” aqueous suspensions via hydrogen reduction. *Journal of Physical Chemistry B* 2004; 108: 13948–13956.
36. Mie G: Contributions on the optics of turbid media, particularly colloidal metal solutions. *Annals of Physics* 1908; 25: 377–445.
37. Noguez C: Surface plasmons on metal nanoparticles: the influence of shape and physical environment. *Journal of Physical Chemistry C* 2007; 111: 3806–3819.
38. Yang N and LiW: Mango peel extract mediated novel route for synthesis of silver nanoparticles and antibacterial application of silver nanoparticles loaded onto non-woven fabrics. *Industrial Crops and Products* 2013; 48: 81–88.
39. Andreescu D, Eastman C, Balantrapu K and Goia DV: A Simple route for manufacturing highly dispersed silver nanoparticles. *Journal of Materials Research* 2007; 22: 2488–2496.
40. FayazAM, Balaji K, Kalaichelvan PT and Venkatesan R: Fungal based synthesis of silver nanoparticles-an effect of temperature on the size of particles. *Colloids and Surfaces B: Bio-interfaces* 2009; 74: 123–126.
41. Pimprikar PS, Joshi SS, Kumar AR, Zinjarde SS and Kulkarni SK: Influence of biomass and gold salt concentration on nanoparticle synthesis by the tropical marine yeast *Yarrowia lipolytica* NCIM 3589. *Colloids and Surfaces B: Biointerfaces* 2009; 74: 309–316.
42. Bar H, Bhui DK, Sahoo GP, Sarkar P, De SP and Misra A: Green synthesis of silver nanoparticles using latex of *Jatropha curcas*. *Colloids and Surfaces A: Physico-chemical and Engineering Aspects* 2009; 339: 134–139.
43. Gardea-Torresedey JL, Gombez G, Jose-Yaceman M, Parsons JG, Peralta-Videa JR and Tioani Jose-Yacaman M: *Alfalfa* Sprouts: A Natural Source for the Synthesis of Silver Nanoparticles. *Langmuir* 2003; 19: 1357–1361.
44. Chwalibog A, Sawosz E, Hotowy A, Szeliga J, Mitura S, Mitura K, Grodzik M, Orlowski P, and Sokolowska A: Visualization of interaction between inorganic nanoparticles and bacteria or fungi. *International Journal of Nanomedicine* 2010; 5: 1085–1094.
45. Prashanth S, Menaka I, Mutheszilan R and Navin KS: Synthesis of plant-mediated silver nano particles using medicinal plant extract and evaluation of its anti microbial activities. *International Journal of Engineering Science and Technology* 2011; 8: 6235–6250.
46. Kim JS, Kuk E, Yu KN, Kim JH, Park SJ, Lee HJ, Kim SH, Park YK, Park YH, Hwang CY, Kim YK, Lee YS, Jeong DH and Cho MH: Antimicrobial effects of silver nanoparticles. *Nanomedicine: Nanotechnology, Biology and Medicine* 2007; 3: 95–101.
47. Bindhu MR and Umadevi M: Synthesis of mono dispersed silver nanoparticles using *Hibiscus cannabinus* leaf extract and its antimicrobial activity. *Spectrochimica Acta Part A: Molecular and Biomolecular Spectroscopy* 2013; 101: 184–190.
48. Li WR, Xie XB, Shi QS, Duan SS, Ou Yang YS and Chen YB: Antibacterial effect of silver nanoparticles on *Staphylococcus aureus*. *Biometals* 2011; 24: 135–141.

49. Song HY, Ko KK, Oh LH and Lee BT: Fabrication of silver nanoparticles and their antimicrobial mechanisms. *European Cells and Materials* 2006; 11: 58.
50. Matsumura Y, Kuniaki Y, Kunisaki SI and Tsuchido T: Mode of Bactericidal Action of Silver Zeolite and Its Comparison with That of Silver Nitrate. *Applied and Environmental Microbiology* 2002; 69: 4278–4281.
51. Pal S, Tak YK and Song JM: Does the Antibacterial Activity of Silver Nanoparticles Depend on the Shape of the Nanoparticle? A Study of the Gram-Negative Bacterium *Escherichia coli*. *Applied and Environmental Microbiology* 2007; 73: 1712–1720.

**How to cite this article:**

Hulkoti NI and Taranath TC: Phyto-fabrication of silver nanoparticles by different physico-chemical parametres using *Petrea volubilis* linn. Leaf broth and evaluation of their anti-microbial activity. *Int J Pharm Sci Res* 2017; 8(10): 4261-72.doi: 10.13040/IJPSR.0975-8232. 8(10). 4261-72.

All © 2013 are reserved by International Journal of Pharmaceutical Sciences and Research. This Journal licensed under a Creative Commons Attribution-NonCommercial-ShareAlike 3.0 Unported License.

This article can be downloaded to **ANDROID OS** based mobile. Scan QR Code using Code/Bar Scanner from your mobile. (Scanners are available on Google Playstore)